Improved clipped periodic optimal control for semi-active harmonic disturbance rejection

Maxime Couillard, Philippe Micheau, Patrice Masson*

G.A.U.S., Mechanical Engineering Department, Université de Sherbrooke, 2500 blvd Universite, Sherbrooke, Québec, Canada J1K 2R1

Abstract

This paper presents a new approach for harmonic disturbance rejection using semi-active vibration control. The approach is illustrated through application to the problem of maximizing the energy dissipated by a semi-active damper under harmonic excitation. In order to establish a baseline for the evaluation of the performance of the semi-active damper, the effectiveness of the optimal passive and active cases are first presented. The study then examines the ability of the clipped optimal control (or clipping control) approach to improve the energy dissipation capacity of the semi-active damper over the optimal passive damper. An approximate solution to the nonlinear dynamic problem, obtained using the method of averaging, and a time integration based numerical method indicate that this approach improves the energy dissipated by the semi-active damper over the optimal passive damper. The approach presented in this paper intends to further "improve", or "fine tune", the control parameters given by the clipped optimal control approach. This is done using an approximated solution of the problem and an appropriate optimization algorithm. Results clearly indicate that this new approach provides significant improvement on energy dissipation over the clipped optimal control approach for the semi-active damper.
© 2008 Elsevier Ltd. All rights reserved.

1. Introduction

The damping of mechanical vibrations is critical in many engineering applications and thus, there exist a vast number of vibration control methods. Vibration control methods can be classified as either being passive, active or semi-active. The main property of a passive method is that it changes the dynamics of a system in an appropriate manner which does not vary as a function of time. Examples of common passive methods are hydraulic dampers, vibration absorbers and viscoelastic damping treatments for flexible structures (for more examples, see Refs. [1,2]). What can be viewed as the counterpart of passive vibration control is the active vibration control which essentially makes use of fully active actuators to either inject or dissipate energy in the system so as to cancel undesirable vibrations. There has been much research on the active control of vibrations in the past decades. Active control methods include, for example, active piezoelectric engine mounts and distributed piezoelectric transducers for flexible structures (for a detailed discussion on the active control of vibrations, see Ref. [3]).

---

*Corresponding author. Tel.: +1 819 821 8000x62152; fax: +1 819 821 7163.

E-mail address: Patrice.Masson@USherbrooke.ca (P. Masson).

Nomenclature

Single degree of freedom system

SDOF   single degree of freedom
ΔE energy dissipated per cycle by the damper
ω frequency of the harmonic excitation
ω_n natural frequency of the SDOF system
τ dimensionless time
ζ damping ratio of the SDOF system
ζ_p damping ratio provided by the damper
ζ_{sa} damping ratio provided by the semi-active damper
$\hat{\zeta}_p$ optimal passive damping ratio of the damper
ζ_{max} maximal damping ratio provided by the semi-active damper
γ normalized maximal damping ratio provided by the semi-active damper
c viscous damping of the SDOF system
c_p viscous damping provided by the damper
c_{sa} viscous damping provided by the semi-active damper
c_{max} maximal viscous damping provided by the semi-active damper
F_{ex} amplitude of the harmonic excitation
k stiffness of the SDOF system
m mass of the SDOF system
r frequency ratio of the excitation
t time
X amplitude of the steady-state displacement of the SDOF system
x displacement of the SDOF system
X_{ex} amplitude of the normalized harmonic excitation

Control system

POC   periodic optimal control
CPOC   clipped periodic optimal control

ICPOC   improved clipped periodic optimal control
β phase of the normalized requested effort
$\hat{\beta}$ phase of the normalized requested effort for the POC and the CPOC
$\tilde{\beta}$ phase of the normalized requested effort for the ICPOC
J cost function
u requested effort
$\hat{u}$ requested effort for the POC and the CPOC
$\tilde{u}$ requested effort for the ICPOC
X_u amplitude of the normalized requested effort
$\hat{X}_u$ amplitude of the normalized requested effort for the POC and the CPOC
$\tilde{X}_u$ amplitude of the normalized requested effort for the ICPOC
x_u normalized requested effort
$\hat{x}_u$ normalized requested effort for the POC and the CPOC
$\tilde{x}_u$ normalized requested effort for the ICPOC

Averaging technique

ϕ time base used for integration in the method of averaging
ψ phase of the averaged motion
θ dimensionless time at which the requested effort gets within the damper's capacity
a amplitude of the averaged motion

A relatively new method, which has also been a subject of research in recent years (see, for example, Refs. [4–12]), is called the semi-active control of vibrations and can be viewed as being halfway between passive and active control. Semi-active control includes methods for which energy is used to change the damping or stiffness of a device appended to a mechanical system. Examples of such methods are: variable orifice hydraulic dampers [13], magneto-rheological vibration absorbers [14] and shunted piezoelectric transducers for flexible structures [15]. Semi-active control is interesting in a number of applications essentially because it can deliver better performance than passive control with a fraction of the power consumption, and thus cost, associated with active control. It is used in a wide variety of applications which includes vibration isolation of equipment [4,5], shock and vibration absorption in transportation [6–8], vibration mitigation in civil engineering [9–11] and many others.

A large part of the research on semi-active control has been devoted to transient and broadband excitation since practical implementations of semi-active control methods are mainly focused around seismic isolation and suspension systems for transportation. Several approaches exist in the literature to synthesize an effective control logic for both kinds of excitation. These approaches mainly originate from the adaptation of active control laws, such as clipped-LQR control [16,17], from nonlinear control approaches, such as sliding mode control [18] and Lyapunov's direct method [12] or simply from physical interpretations (see skyhook and groundhook control in Ref. [11]). In contrast, there has been little effort to exploit harmonic disturbance rejection using semi-active control even if many vibration control problems are harmonic in nature [4]. Moreover, the effectiveness of the control approaches proposed for transient and broadband excitation have limited performance on harmonic disturbance rejection since they mainly originate from either infinite time horizon optimization (as for LQR approaches) or instantaneous time horizon optimization (as for sliding mode control and Lyapunov's direct method). To really design a control law focused on periodic disturbance rejection, a periodic time horizon optimization has to be considered [19].

As one of the few papers specifically oriented toward harmonic disturbance rejection, Anusonti-Inthra and Gandhi [4] proposed an interesting approach for the semi-active isolation problem using a frequency domain control algorithm at twice the frequency of the excitation. In order to ensure the compatibility of their control algorithm with their damper, they implemented a "scaled down" version of their active optimal control law. The process of "scaling down" the control can be viewed as to apply a penalty on the requested effort so that it is always lower or equal to what the damper can provide. Although their system is clearly effective, the effect of "scaling down" the active optimal control is not thoroughly discussed. Liu et al. [20] have also studied the semi-active harmonic isolation problem by comparing four different already established physical interpretation based semi-active control laws. A good example of a *physical interpretation based control law* is the "skyhook" control, where the control law intends to emulate a viscous damper connected between the sky and the mass. Although effective, control laws arising from physical interpretations do not take a periodic time horizon optimization into account. Also, experimental work has been done by Buaka et al. [21] on a semi-active friction device controlled by a Bang–Bang control based on Lyapunov's direct method. They showed that with proper control parameters and phase-shift compensation, it was possible to improve the energy dissipated by their semi-active damper over a strictly passive damper under harmonic excitation. However, Lyapunov's direct method is based on an instantaneous time horizon optimization and thus, it is not specifically intended for harmonic disturbance rejection. Pinkaew and Fujino [17] studied the effectiveness of a semi-active tuned mass damper under harmonic excitation controlled by a clipped-LQR control law. Again, the approach is not specifically oriented toward harmonic disturbance rejection since the control is based on an infinite time horizon optimization. However, they showed that clipping an LQR control law essentially leads to the minimization of the instantaneous increasing cost from the cost function of the corresponding optimal active system. This means that by clipping an LQR control, one loose the infinite time horizon optimality.

A review of the literature for semi-active harmonic disturbance rejection tends to indicate that semi-active control can achieve better results than passive control in practically every situation. But most of the control laws used are either "clipped" or "scaled down" versions of active optimal control laws or control laws arising from nonlinear approaches or physical interpretations that do not take the periodicity of the phenomenon into account. Moreover, for the control laws that do take the periodicity of the phenomenon into account [4], further investigation is required on the effect of clipping (or even scaling down) the active optimal control to respect the inherent passivity (no energy injected) and the modulation capacity of the semi-active damper.

2. Objective and methodology

This paper proposes a new approach allowing to obtain an effective control law for harmonic disturbance rejection. In order to illustrate the approach, it focuses on the following problem: given the semi-actively damped single degree of freedom (SDOF) system in Fig. 1(b), derive a semi-active control law in order to maximize the energy dissipated per cycle by the semi-active damper. Recognizing the difficulty of finding the true "semi-active optimal control law" for this nonlinear optimization problem, a simple approach is

proposed, based on an approximated solution to the nonlinear dynamic problem, in order to derive an appropriate control law.

It is important to understand that the idea of maximizing the energy dissipated by the semi-active damper is not the same as to minimize the response of the system's mass, in which case it would be more effective to reduce the work done on the mass in the first place. The results presented in this paper are thus mostly of theoretical interest. However, on a practical point of view, the method could be useful for researchers interested in the field of energy harvesting (see, for example, Ref. [22]).

The *clipped optimal control* (or *clipping control*) approach [11] is used as a starting point. This method essentially involves two steps. The first step is to determine the fully active control law that optimizes the chosen cost function. For the problem considered in this paper, this has been done by Kasturi and Dupont [19] and the result will be briefly recalled in Section 3 along with the optimal passive case. The second step is then to design the clipping controller that will best reproduce the active optimal effort, while respecting the inherent passivity (no energy injected) and the modulation capacity of the semi-active damper. This second step yields the "clipped optimal control law" and will be the subject of Section 4. The originality of this paper is to propose to add a third step to this approach, which can be viewed as "improving" or "fine tuning" the clipped optimal control law. The improvement of the clipped optimal control law is done using an approximate solution to the nonlinear dynamic problem and an appropriate optimization algorithm, which will be discussed in Section 5. It will be shown that this third step leads to considerable improvement over clipped optimal control laws used for semi-active harmonic disturbance rejection.

3. Passive and active damping optimization

This section aims at establishing the optimal energy dissipated for both a passive viscous damper and a fully active damper under harmonic excitation. This will be used as a baseline to assess the performance of the semi-active damper against its passive and active counterparts. Note that the active control law will also serve as the basis for the design of the control laws presented in Sections 4 and 5.

3.1. Passive viscous damping optimization

Consider the damped SDOF system with an added viscous damping provided by a passive damper as shown in Fig. 1(a). It can be logically inferred that for a value of added passive damping of zero, no energy will be dissipated and that for a value of added passive damping that tends toward infinity, no energy will be dissipated either since the response of the system will be infinitely small. Thus, we can assume that there is an optimal value of damping that will maximize energy dissipation which lies between zero and infinity. The purpose of this section is to compute that optimal value. The equation of motion of the system under
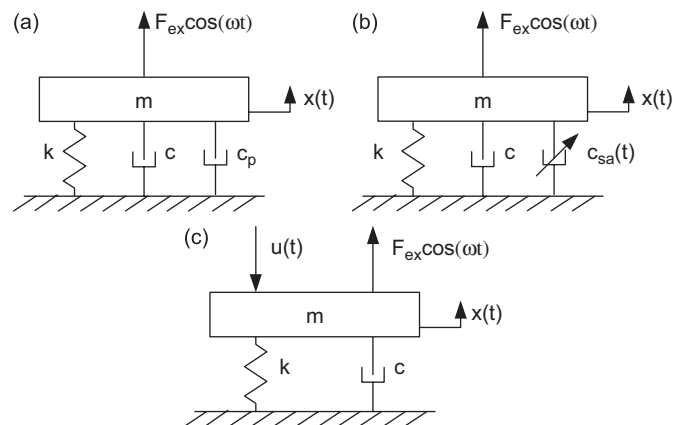

Fig. 1. SDOF system with an added: (a) passive viscous damper, (b) semi-active viscous damper and (c) active damper.

harmonic excitation is

$$m\ddot{x} + (c + c_p)\dot{x} + kx = F_{\text{ex}}\cos\omega t, \tag{1}$$

which can be rewritten in dimensionless form such as

$$\ddot{x} + 2(\zeta + \zeta_p)\omega_n\dot{x} + \omega_n^2 x = \omega_n^2 X_{\text{ex}}\cos\omega t, \tag{2}$$

where $\omega_n = \sqrt{k/m}$, $\zeta = c/(2m\omega_n)$, $\zeta_p = c_p/(2m\omega_n)$ and $X_{\text{ex}} = F_{\text{ex}}/k$. It can be shown that the amplitude of the motion under steady state is [1]

$$X = \frac{X_{\text{ex}}}{\sqrt{(1 - r^2)^2 + (2(\zeta + \zeta_p)r)^2}}, \tag{3}$$

where $r = \omega/\omega_n$. The energy dissipated by the damper is found by integrating the *damping force × distance* product over one cycle so that

$$\Delta E = 2\pi k r \zeta_p X^2. \tag{4}$$

The added passive damping that maximizes Eq. (4) is solution of $\mathrm{d}\Delta E/\mathrm{d}\zeta_p = 0$ since $\mathrm{d}^2\Delta E/\mathrm{d}\zeta_p^2 < 0$. Extracting only the positive root, this yields the optimal added damping ratio:

$$\hat{\zeta}_p = \frac{\sqrt{(1 - r^2)^2 + (2\zeta r)^2}}{2r}. \tag{5}$$

Using Eqs. (3)–(5), the closed-form expression of the energy dissipated per cycle, under steady-state regime, by the optimal added viscous damping for harmonic excitation is obtained:

$$\Delta E = \frac{\pi k X_{\text{ex}}^2}{2\left(\sqrt{(1 - r^2)^2 + (2\zeta r)^2} + 2r\zeta\right)}. \tag{6}$$

Discussion on this result is left to Section 3.3.

3.2. Active damping optimization

The system shown in Fig. 1(c), where the damping is provided by an active effort, u, is now considered. The dimensionless equation of motion of this system is

$$\ddot{x} + 2\zeta\omega_n\dot{x} + \omega_n^2(x + x_u) = \omega_n^2 X_{\text{ex}}\cos\omega t, \tag{7}$$

where $x_u = u/k$. As opposed to the static optimization problem of the preceding section, optimizing the energy dissipated by the control effort is in this case a dynamic optimization problem in which the cost function to be minimized is

$$J(u) = \int_{t_0}^{t_0 + 2\pi/\omega} -u\dot{x}\,\mathrm{d}t. \tag{8}$$

With regards to linear optimal control theory, this problem is called a singular problem since the derivative of the Hamiltonian to the control effort, $\partial H/\partial u$, does not yield an implicit expression of u. There is no prescribed method to solve this kind of problem and thus specific solutions are obtained for specific cases. Kasturi and Dupont [19] were able to give a closed-form solution to this problem for the case of any periodic excitation using a standard variational approach. For the case of an harmonic excitation as in Fig. 1(c), with $t_0 = 0$, the normalized active optimal requested effort and the energy dissipated per cycle at this optimal effort become

$$\hat{x}_u(t) = \hat{X}_u\cos(\omega t - \hat{\beta}), \tag{9}$$

$$\Delta E = \frac{\pi k X_{\text{ex}}^2}{8\zeta r}, \tag{10}$$

where the amplitude and phase of $\hat{x}_u$ are, respectively,

$$\hat{X}_u = \frac{X_{ex}}{2}\sqrt{1 + \left(\frac{r^2 - 1}{2\zeta r}\right)^2}, \tag{11}$$

$$\hat{\beta} = \tan^{-1}\left(\frac{r^2 - 1}{2\zeta r}\right). \tag{12}$$

This is an open-loop control that will be referred to as the "periodic optimal control" (POC). For a detailed discussion on the POC, the reader is referred to the paper by Kasturi and Dupont [19].

3.3. Optimal passive damping versus optimal active damping

From the comparison of optimal passive damping with optimal active damping, two observations can be made:

(1) The energy dissipated per cycle at optimal by the active and passive dampers (see Eqs. (6) and (10)) is proportional to kX_{ex}^2. In order to provide a dimensionless result, the energy dissipated per cycle will be expressed as the *normalized energy dissipated per cycle* ($= \Delta E/(kX_{ex}^2)$) in the following.
(2) For $r = 1$, the optimal energy dissipated per cycle by the active and passive dampers (see Eqs. (6) and (10)) become equal so that there is no gain to be made by using an active damping force over a passive one. This can be explained by the fact that, at this point, $\hat{\beta}$ vanishes so $\hat{x}_u$ has a phase opposite to the one of the excitation (remember from Fig. 1(c) that they act in opposite direction) and thus, this is equivalent to passive viscous damping.

To better illustrate the results presented in this section, a plot of the regions delimited by the passive and active normalized energy dissipated per cycle at optimal is presented in Fig. 2 for $\zeta = 5.63$ percent. The SDOF parameters used throughout this paper are based on the semi-active device presented by Buaka [23] ($m = 0.228$ kg, $\zeta = 5.63$ percent, $k = 17\,500$ N/m) with $F_{ex} = 2$ N. Fig. 2 allows to distinguish three distinct regions of performance, which are:

(1) The region with a performance inferior to an optimal passive damper. If the performance of the semi-active damper falls in this region, this means the control law offers no advantages compared to a passive damper.
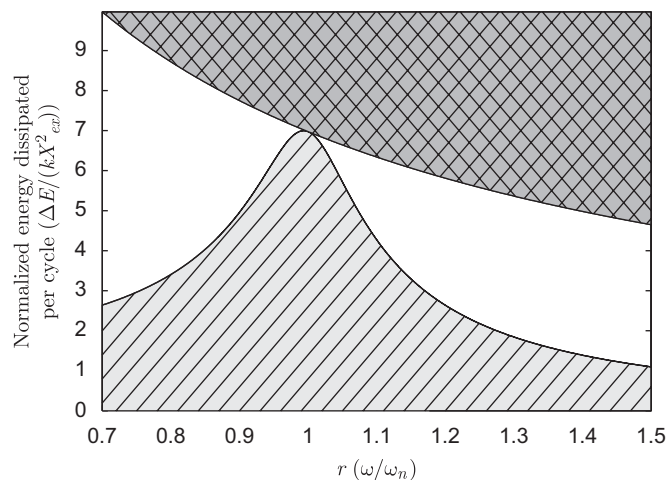

Fig. 2. Possible regions of operation for the semi-active viscous damper: (▨) region with a performance inferior to an optimal passive damper; (▢) region with a performance superior to an optimal passive damper and inferior to an optimal active damper; (▧) region with a performance superior to an optimal active damper.

(2) The region with a performance superior to an optimal passive damper and inferior to an optimal active damper. This is the expected region of operation of the semi-active damper.
(3) The region with a performance superior to an optimal active damper. It is expected that this region is unattainable since theoretically, no semi-active control can achieve better performance than an optimal active control when considering the same cost function.

4. Clipped periodic optimal control

The purpose of this section is to evaluate the capacity of the *clipped optimal control* (or *clipping control*) approach [11] to improve, over the optimal passive case, the energy dissipated per cycle by a semi-active damper under harmonic excitation. Therefore, this section is focused on the design of a clipped version of the POC presented in Section 3.2, which will be called the "clipped periodic optimal control" (CPOC) in the following.

4.1. Design of the CPOC

Before proceeding to the design of the CPOC, a new parameter is introduced that will allow to do a fair comparison between the semi-active damper and the passive damper. This new parameter, which will be called the normalized maximal allowed damping, noted γ, is defined as being the ratio of the maximal allowed damping ratio of the semi-active damper, ζ_{max}, to the optimal damping ratio of the passive damper, $\hat{\zeta}_p$, as expressed by Eq. (5), such as

$$\gamma = \frac{\zeta_{max}}{\hat{\zeta}_p}. \tag{13}$$

This essentially means that, by setting γ, we will allow ζ_{max} to vary with the frequency ratio, so it is always in the same proportion with respect to $\hat{\zeta}_p$.

For the design of the CPOC, consider the case of the SDOF system damped by a semi-active viscous damper as shown in Fig. 1(b). The difference between Fig. 1(a) and (b) is that the added damping to the system now
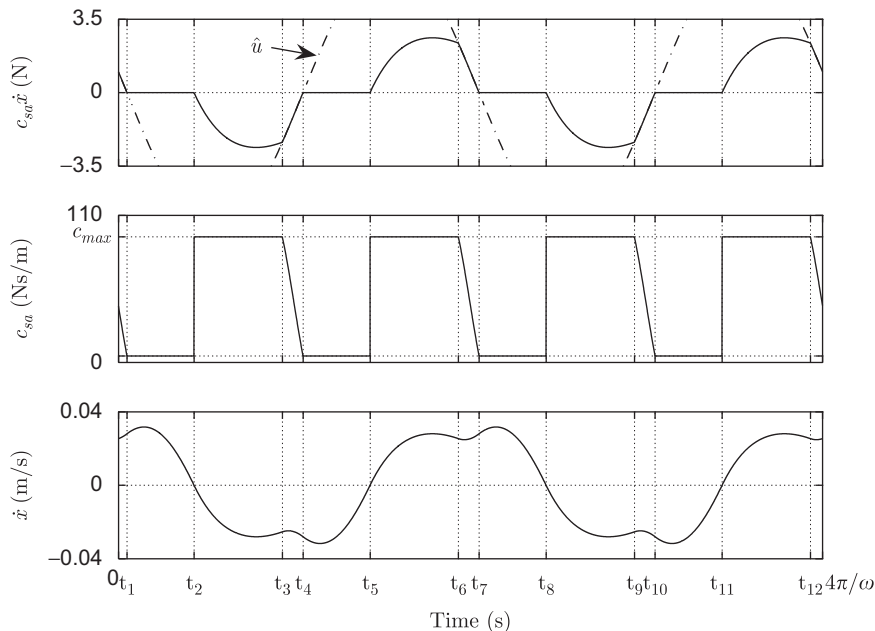

Fig. 3. Time history of the CPOC for $r = 0.7$ and $\gamma = 2$ (t_i indicates a change of mode of operation).

becomes a function of time and it can only lie in the interval $0 \leqslant \zeta_{\text{sa}}(t) \leqslant \zeta_{\max}$. The idea behind the control approach of the CPOC is that it will try to reproduce $\hat{x}_u$, in an instantaneous sense, by modulating ζ_{sa}. Since the semi-active damper cannot inject energy into the system and has a limited maximal effort, it can be logically inferred that the CPOC will yield a control law that will have three distinct "modes" of operation. To better illustrate this affirmation, time based simulations of the CPOC for $\gamma = 2$ are shown for $r = 0.7$ in Fig. 3,
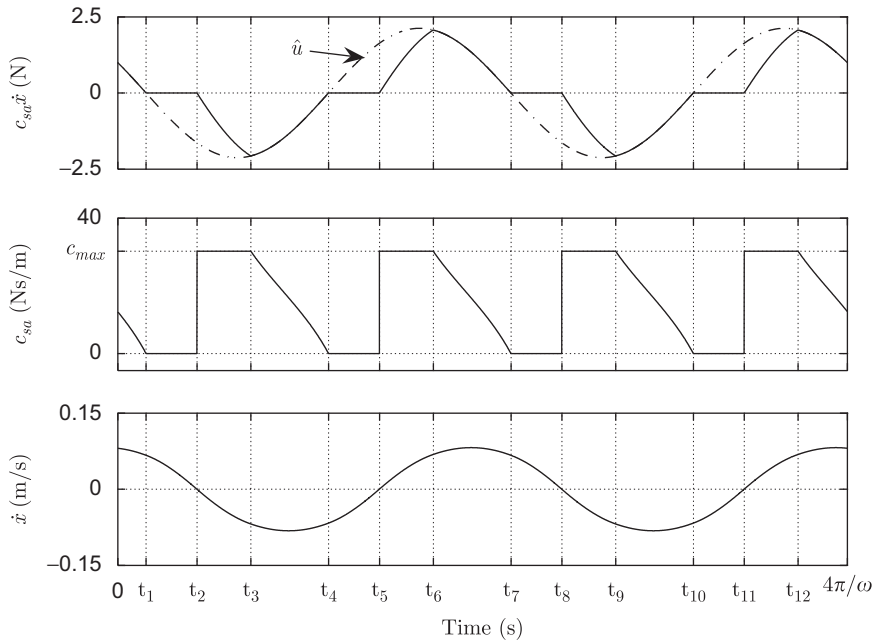

Fig. 4. Time history of the CPOC for $r = 0.9$ and $\gamma = 2$ (t_i indicates a change of mode of operation).
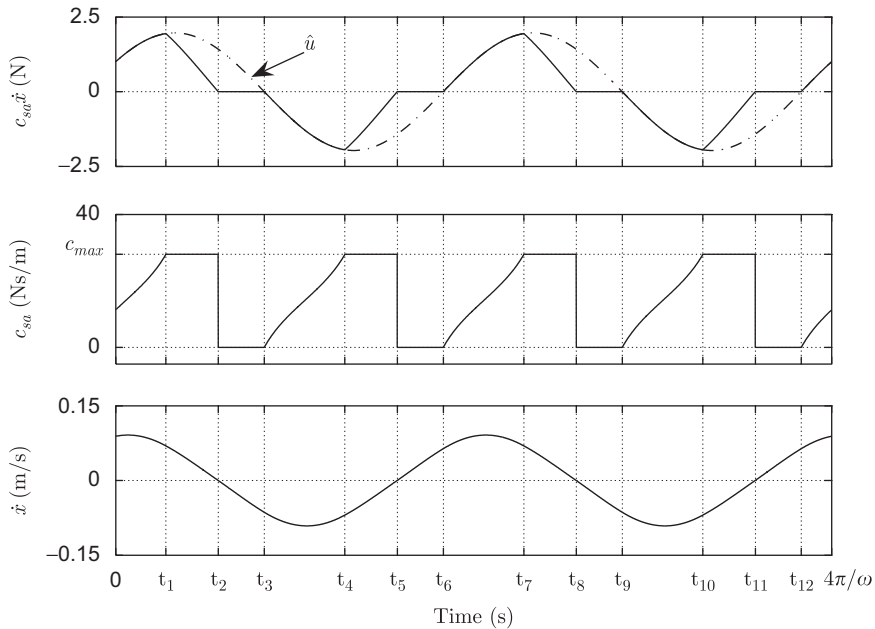

Fig. 5. Time history of the CPOC for $r = 1.1$ and $\gamma = 2$ (t_i indicates a change of mode of operation).
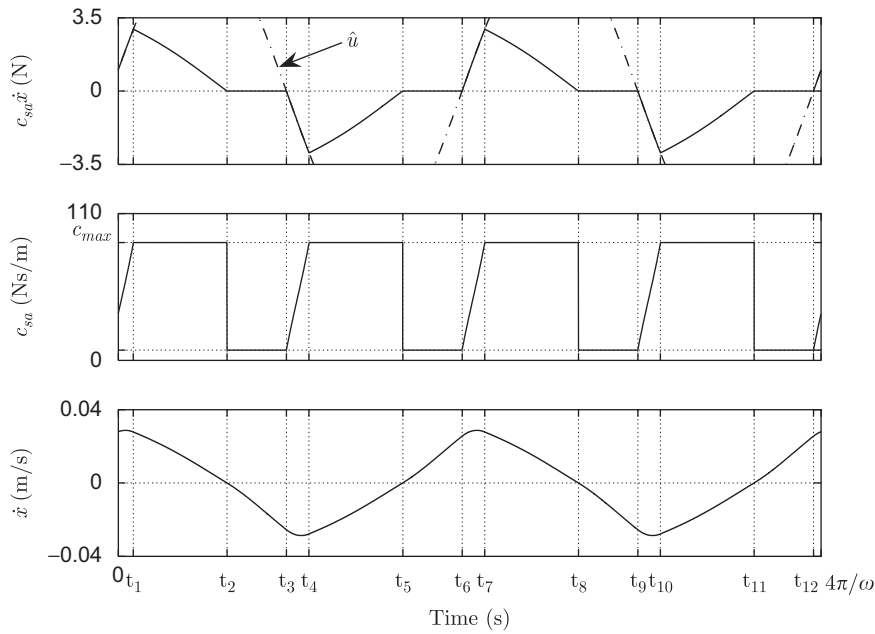
Fig. 6. Time history of the CPOC for $r = 1.5$ and $\gamma = 2$ (t_i indicates a change of mode of operation).

for $r = 0.9$ in Fig. 4, for $r = 1.1$ in Fig. 5 and for $r = 1.5$ in Fig. 6. The three distinct "modes" of operation of the semi-active damper can be defined as follows:

(1) When $\hat{u}$ opposes the velocity and is within the effort the damper can provide, c_{sa} is adjusted so that $c_{sa}\dot{x} = \hat{u}$ or, in dimensionless form, ζ_{sa} is adjusted so that $\zeta_{sa}\dot{x} = \omega_n \hat{x}_u/2$. Examples of such cases are the time intervals $t_3 \leqslant t \leqslant t_4$ in Figs. 3–6.
(2) When $\hat{u}$ opposes the velocity but is greater than the effort the damper can provide, the damping is held at c_{max}, or, in dimensionless form, $\zeta_{sa} = \zeta_{max}$. Examples of such cases are the time interval $t_2 \leqslant t < t_3$ in Figs. 3 and 4 and the time interval $t_1 < t \leqslant t_2$ in Figs. 5 and 6.
(3) When $\hat{u}$ is in the same direction as the motion, so that it would inject energy into the system, the semi-active damper is set at the lowest amount of damping it can produce, which, for simplicity, will be considered here to be $c_{sa} = 0$ (or $\zeta_{sa} = 0$). Examples of such cases are the time interval $t_1 < t < t_2$ in Figs. 3 and 4 and the time interval $t_2 < t < t_3$ in Figs. 5 and 6.

Therefore, the preceding control law can be represented, in its dimensionless form, by the following equation:

$$\zeta_{sa} = \begin{cases} \dfrac{\omega_n \hat{x}_u}{2\dot{x}} & \text{if } \hat{x}_u \dot{x} \geqslant 0 \ \text{ and } \ \dfrac{\omega_n \hat{x}_u}{2\dot{x}} \leqslant \zeta_{max}, \\[2ex] \zeta_{max} & \text{if } \hat{x}_u \dot{x} \geqslant 0 \ \text{ and } \ \dfrac{\omega_n \hat{x}_u}{2\dot{x}} > \zeta_{max}, \\[2ex] 0 & \text{otherwise.} \end{cases} \tag{14}$$

4.2. Approximate steady-state solution using the method of averaging

This section aims at establishing an approximate solution to the nonlinear dynamic problem of the semi-actively damped SDOF system controlled with the CPOC. This is done in order to obtain some analytical insights to the problem and also to validate the results from time based simulations. The approximate solution

to the CPOC problem is obtained using the method of averaging. As illustrated by Shen et al. [6], this method can be applied to semi-active vibration control problems in order to obtain an approximated frequency response function of the system.

The first step in the averaging method analysis is to write the equation of motion of the system in its dimensionless form, introducing dimensionless time $\tau = \omega t$:

$$r^2 \frac{\mathrm{d}^2 x}{\mathrm{d}\tau^2} + 2(\zeta + \zeta_{\mathrm{sa}})r \frac{\mathrm{d}x}{\mathrm{d}\tau} + x = X_{\mathrm{ex}} \cos \tau. \tag{15}$$

Applying the *first-order* method of averaging, we seek a solution in the form

$$x = a(\tau) \cos \phi(\tau), \tag{16}$$

$$\frac{\mathrm{d}x}{\mathrm{d}\tau} = -a(\tau) \sin \phi(\tau), \tag{17}$$

where $\phi(\tau) = \tau + \psi(\tau)$. Note that the amplitude and phase of the motion, a and ψ, are considered to be slowly varying functions of τ. Differentiating Eq. (16) with respect to r and requiring Eq. (17) to hold, we obtain

$$\frac{\mathrm{d}a}{\mathrm{d}\tau} \cos \phi - a \frac{\mathrm{d}\psi}{\mathrm{d}\tau} \sin \phi = 0. \tag{18}$$

Differentiating Eq. (17) with respect to τ and substituting the results in Eq. (15) yields

$$a\left(1 - r^2 - r^2 \frac{\mathrm{d}\psi}{\mathrm{d}\tau}\right) \cos \phi - \left(r^2 \frac{\mathrm{d}a}{\mathrm{d}\tau} + 2(\zeta + \zeta_{\mathrm{sa}})ar\right) \sin \phi = X_{\mathrm{ex}} \cos(\phi - \psi). \tag{19}$$

Eqs. (18) and (19) can then be solved for $\mathrm{d}a/\mathrm{d}\tau$ and $\mathrm{d}\psi/\mathrm{d}\tau$ so that

$$2r^2 \frac{\mathrm{d}a}{\mathrm{d}\tau} = a(1 - r^2) \sin 2\phi - 4(\zeta + \zeta_{\mathrm{sa}})ar \sin^2\phi - 2X_{\mathrm{ex}} \sin \phi \cos(\phi - \psi), \tag{20}$$

$$2ar^2 \frac{\mathrm{d}\psi}{\mathrm{d}\tau} = 2a(1 - r^2) \cos^2\phi - 2(\zeta + \zeta_{\mathrm{sa}})ar \sin 2\phi - 2X_{\mathrm{ex}} \cos \phi \cos(\phi - \psi). \tag{21}$$

The next step of the method is to obtain an approximate solution of the steady-state response of the system by averaging $\mathrm{d}a/\mathrm{d}\tau$ and $\mathrm{d}\psi/\mathrm{d}\tau$ over one period of time $0 \leqslant \phi \leqslant 2\pi$ such as

$$2r^2 \frac{\mathrm{d}a}{\mathrm{d}\tau} = \frac{1}{2\pi} \int_0^{2\pi} [a(1 - r^2) \sin 2\phi - 4(\zeta + \zeta_{\mathrm{sa}})ar \sin^2\phi - 2X_{\mathrm{ex}} \sin \phi \cos(\phi - \psi)] \, \mathrm{d}\phi, \tag{22}$$

$$2ar^2 \frac{\mathrm{d}\psi}{\mathrm{d}\tau} = \frac{1}{2\pi} \int_0^{2\pi} [(2a - 2ar^2 - 2X_{\mathrm{ex}} \cos \psi) \cos^2\phi - (2(\zeta + \zeta_{\mathrm{sa}})ar + X_{\mathrm{ex}} \sin \psi) \sin 2\phi] \, \mathrm{d}\phi. \tag{23}$$

Note that these are partial integrations in the sense that a and ψ are held fixed during the integration process. This means that the response of the system is assumed to be harmonic. Therefore, in order to solve the integrals of Eqs. (22) and (23), the control law of Eq. (14) can be rewritten in terms of time such as

for $r \leqslant 1$:

$$\zeta_{\mathrm{sa}} = \begin{cases} \zeta_{\max}, & 0 \leqslant \phi < \theta, & \pi \leqslant \phi < \theta + \pi, \\ \dfrac{\omega_n \hat{x}_u}{2\dot{x}}, & \theta \leqslant \phi \leqslant \hat{\beta} + \psi + \pi/2, & \theta + \pi \leqslant \phi \leqslant \hat{\beta} + \psi + 3\pi/2, \\ 0, & \hat{\beta} + \psi + \pi/2 < \phi < \pi, & \hat{\beta} + \psi + 3\pi/2 < \phi < 2\pi. \end{cases} \tag{24a}$$

for $r > 1$:

$$\zeta_{\mathrm{sa}} = \begin{cases} 0, & 0 < \phi < \hat{\beta} + \psi + \pi/2, & \pi < \phi < \hat{\beta} + \psi + 3\pi/2, \\ \dfrac{\omega_n \hat{x}_u}{2\dot{x}}, & \hat{\beta} + \psi + \pi/2 \leqslant \phi \leqslant \theta, & \hat{\beta} + \psi + 3\pi/2, \ \leqslant \phi \leqslant \theta + \pi, \\ \zeta_{\max}, & \theta < \phi \leqslant \pi, & \theta + \pi < \phi \leqslant 2\pi, \end{cases} \tag{24b}$$

where θ is the dimensionless time at which the requested effort gets within the damper's capacity, such as

$$\theta = -\tan^{-1}\left(\frac{\hat{X}_u \cos(\hat{\beta} + \phi)}{\hat{X}_u \sin(\hat{\beta} + \phi) + 2\zeta_{\max} ar}\right). \tag{25}$$

Note that Eq. (24) implies that for $r \leqslant 1$, we will have $a \leqslant 0$ and $0 \leqslant \psi < 2\pi$ and for $r > 1$, we will have $a \geqslant 0$ and $-2\pi < \psi \leqslant 0$. The next step in the method of averaging is then to solve Eqs. (22) and (23) using the control logic of Eq. (24) to obtain the averaged version of $\mathrm{d}a/\mathrm{d}\tau$ and $\mathrm{d}\psi/\mathrm{d}\tau$. This yields

for $r \leqslant 1$:

$$\frac{\mathrm{d}a}{\mathrm{d}\tau} = \frac{1}{4\pi r^2}(2\zeta_{\max} ar \sin 2\theta - \hat{X}_u(2\theta - 2\hat{\beta} - 2\psi - \pi)\sin(\hat{\beta} + \psi) - 4ar(\zeta_{\max}\theta + \zeta\pi)$$
$$+ \hat{X}_u \cos(2\theta - \hat{\beta} - \psi) + \hat{X}_u \cos(\hat{\beta} + \psi) - 2\pi X_{\mathrm{ex}} \sin \psi), \tag{26a}$$

for $r > 1$:

$$\frac{\mathrm{d}a}{\mathrm{d}\tau} = \frac{1}{4\pi r^2}(-2\zeta_{\max} ar \sin 2\theta + \hat{X}_u(2\theta - 2\hat{\beta} - 2\psi - \pi)\sin(\hat{\beta} + \psi)$$
$$+ 4ar(\zeta_{\max}\theta - \zeta_{\max}\pi - \zeta\pi) - \hat{X}_u \cos(2\theta - \hat{\beta} - \psi) - \hat{X}_u \cos(\hat{\beta} + \psi) - 2\pi X_{\mathrm{ex}} \sin \psi), \tag{26b}$$

and for $r \leqslant 1$:

$$\frac{\mathrm{d}\psi}{\mathrm{d}\tau} = \frac{1}{4\pi ar^2}(-\hat{X}_u \sin(2\theta - \hat{\beta} - \psi) - \hat{X}_u(2\theta - 2\hat{\beta} - 2\psi - \pi)\cos(\hat{\beta} + \psi)$$
$$- \hat{X}_u \sin(\hat{\beta} + \psi) - 4ar\zeta_{\max} \sin^2 \theta + 2\pi a(1 - r^2) - 2\pi X_{\mathrm{ex}} \cos \psi), \tag{27a}$$

for $r > 1$:

$$\frac{\mathrm{d}\psi}{\mathrm{d}\tau} = \frac{1}{4\pi ar^2}(\hat{X}_u \sin \sin(2\theta - \hat{\beta} - \psi) + \hat{X}_u(2\hat{\beta} - 2\psi - \pi)\cos(\hat{\beta} + \psi)$$
$$+ \hat{X}_u \sin(\hat{\beta} + \psi) + 4ar\zeta_{\max} \sin^2 \theta + 2\pi a(1 - r^2) - 2\pi X_{\mathrm{ex}} \cos \psi). \tag{27b}$$

Assuming that, at steady state, the amplitude a and the phase ψ are constant so that $\mathrm{d}a/\mathrm{d}\tau = 0$ and $\mathrm{d}\psi/\mathrm{d}\tau = 0$, the final step of the averaging method is to solve Eqs. (26) and (27) for a and ψ. For this particular case, the resulting equations are nonlinear and getting an explicit expression of a and ψ is not possible. Thus, we must rely on a numerical method which can be viewed as an optimization routine that generates an estimate of a and ψ to minimize the cost function of Eq. (28). The optimization routine used in this paper is based on the Nelder–Mead simplex (direct search) method [24].

$$J(a, \psi) = \left[\left(\frac{\mathrm{d}a}{\mathrm{d}\tau}\right)^2 + \left(\frac{\mathrm{d}\psi}{\mathrm{d}\tau}\right)^2\right]. \tag{28}$$

Again, for $r \leqslant 1$, it is expected that $a \leqslant 0$ and $0 \leqslant \psi < 2\pi$ and for $r > 1$, it is expected that $a \geqslant 0$ and $-2\pi < \psi \leqslant 0$. Using a and ψ as given by the preceding optimization routine, the energy dissipated per cycle can be determined by integrating the *damping force* × *distance* product over one cycle. This yields

for $r \leqslant 1$:

$$\Delta E = ka^2 r\zeta_{\max}(2\theta - \sin 2\theta) + ka\hat{X}_u(\theta - \hat{\beta} - \psi)\sin(\hat{\beta} + \psi)$$
$$- \tfrac{1}{2}ka\hat{X}_u(\pi \sin(\hat{\beta} + \psi) + \cos(\hat{\beta} + \psi) + \cos(2\theta - \psi - \hat{\beta})), \tag{29a}$$

for $r > 1$:

$$\Delta E = -ka^2 r\zeta_{\max}(2\theta - 2\pi - \sin 2\theta) - ka\hat{X}_u(\theta - \hat{\beta} - \psi)\sin(\hat{\beta} + \psi)$$
$$+ \tfrac{1}{2}ka\hat{X}_u(\pi \sin(\hat{\beta} + \psi) + \cos(\hat{\beta} + \psi) + \cos(2\theta - \psi - \hat{\beta})), \tag{29b}$$

4.3. Numerical analysis and discussion on the CPOC

This section intends to numerically evaluate the performance of the CPOC using two different methods. The first method is based on the averaged solution of the previous section. The main steps involved in this method are:

(1) define system parameters: m, k, c, c_{max}, ω and F_{ex};
(2) determine the averaged steady-state motion amplitude and phase using an optimization routine on Eqs. (26) and (27) with the cost function of Eq. (28) to be minimized;
(3) evaluate the energy dissipated per cycle using Eq. (29a).

The second method used for the analysis is a time integration based method. Although a time integration based method is quite inefficient in terms of computation time (mainly because it needs to integrate time until steady state is obtained), it is believed that it will give an excellent estimate of the energy dissipated per cycle. The main steps involved in the time integration based method that will be used in the following can be described as follows:

(1) define system parameters: m, k, c, c_{max}, ω and F_{ex};
(2) numerically integrate the equation of motion over 100 cycles in order to obtain a steady-state solution (considering a damping ratio of $\zeta = 5.63$ percent, 100 cycles is considered to be sufficient);
(3) determine the energy dissipated by the semi-active damper by numerically integrating the *damping force × distance* product over one cycle.

Fig. 7 illustrates the normalized energy dissipated per cycle in terms of the frequency ratio obtained from the time integration based method and the averaged solution for $\gamma = 1.25$ and 2. The plot clearly shows that the CPOC can improve the energy dissipated per cycle by a semi-active damper compared to an optimal passive damper and this, over the entire span of frequency ratio considered. This is in agreement with the literature where, generally speaking, clipped optimal controls have been shown to provide increased performance over strictly passive systems (see, for example, Refs. [16,17,25]). Moreover, if the maximal allowed damping provided by the semi-active damper is increased, by increasing γ from 1.25 to 2, the energy dissipated per cycle is also increased, as intuition would suggest. It is also expected that as ζ is reduced, the potential for energy dissipation will be increased as it is the case for the passive and active dampers.
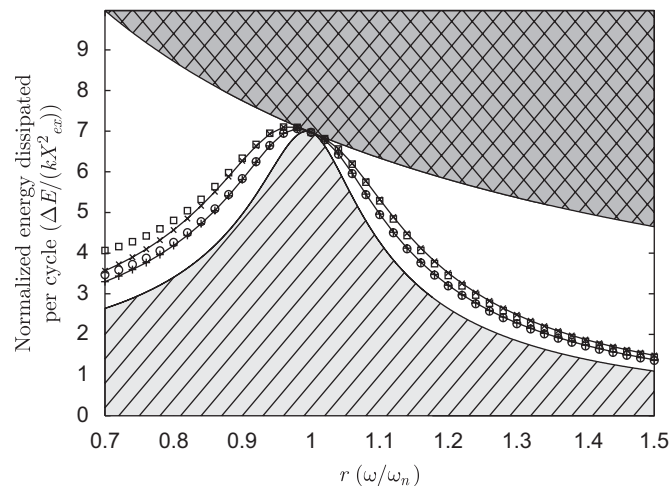

Fig. 7. Normalized energy dissipated per cycle in terms of the frequency ratio obtained for the CPOC from the time integration based method and the averaged solution: (○) time integration for $\gamma = 1.25$; (——+——) averaged solution for $\gamma = 1.25$; (□) time integration for $\gamma = 2$; (——×——) averaged solution for $\gamma = 2$.

Another interesting feature of the CPOC, as it can be seen in Figs. 3–6, is that it yields a control effort, $c_{sa}\dot{x}$, that is periodic at twice the frequency of excitation. This control is therefore coherent with the paper presented by Anusonti-Inthra and Gandhi [4] where they designed a frequency domain controller at twice the frequency of the excitation.

As for the ability of the averaged solution to evaluate the energy dissipated per cycle by the CPOC under steady state compared to the time integration based method, we can see that in the vicinity of $r = 1$, the agreement between both methods is excellent. However, the agreement tends to deteriorate as the frequency ratio gets away from $r = 1$ and as γ is increased. This is essentially because the motion gets distorted and the harmonic motion assumption becomes less acceptable. However, the agreement between both methods is considered satisfactory.

5. Improved clipped periodic optimal control

Although the CPOC presented in Section 4 was shown to be effective, it must be emphasized that clipping an active optimal control law does not guarantee "semi-active optimality" in any way. For the problem considered here, this means that there is no guarantee that clipping an harmonic requested effort is "semi-active optimal" and even less that $\hat{X}_u$ and $\hat{\beta}$ are the harmonic requested effort optimal parameters. Because of the nonlinear nature of the problem and therefore the inherent difficulty of finding the true "semi-active optimal" control, this paper proposes to rather "improve" or "fine tune" the solution given by the clipped optimal control approach. In that sense, the same control law as with the CPOC will be used but with a new normalized requested effort, noted $\tilde{x}_u$, that will yield larger energy dissipation than $\hat{x}_u$. This new control will be called the "improved clipped periodic optimal control" (ICPOC). It will be shown that the ICPOC can give considerable gains on energy dissipation over the CPOC.

5.1. Design of the ICPOC

To better understand the objectives of this section, we first rewrite Eq. (9) using complex exponential notation so that

$$\hat{x}_u(t) = \left(\frac{X_{ex}}{2} - j(r^2 - 1)\frac{X_{ex}}{4\zeta r} \right) e^{j\omega t}. \tag{30}$$

Eq. (30) shows that the POC indicates an optimal point in the complex plane. To illustrate this, Figs. 8 and 9 present contour plots of the normalized energy dissipated per cycle in terms of the real and imaginary parts of x_u, for both the active and the semi-active cases. These plots were obtained using the time integration based procedure presented in Section 4.3 and discretizing the complex plane in a relatively fine mesh (61×61 points). Fig. 8 clearly shows that, for the active case, the location given by $\hat{x}_u$ is on an optimal point in the complex plane. On the other hand, Fig. 9 shows that the location given by $\hat{x}_u$ is clearly not at an optimal point in the complex plane for the semi-active case.

The purpose of this section will be to find that optimal point, given by $\tilde{x}_u$, assuming that it exists.

It is also interesting to point out that the plot for the active damper presented in Fig. 8 allows negative values for energy dissipation, which is not the case for the plot for the semi-active damper presented in Fig. 9. This is coherent with the fact that the active damper can inject energy into the system while this is impossible for the semi-active damper. Note, however, that the optimal point of Fig. 8 does represent a positive value for energy dissipation.

5.2. Assessment of the averaged solution for the ICPOC

Section 4.2 presented an averaged solution for the CPOC, in which case $\hat{x}_u$ represented the requested effort to the semi-active damper. Since we are using the same control law as with the CPOC but with a different requested effort, one might wonder if it would be possible to use the same averaged solution while varying x_u in order to find $\tilde{x}_u$. (Note: in that case, $\tilde{x}_u$ will represent the optimal form of x_u for the averaged solution but
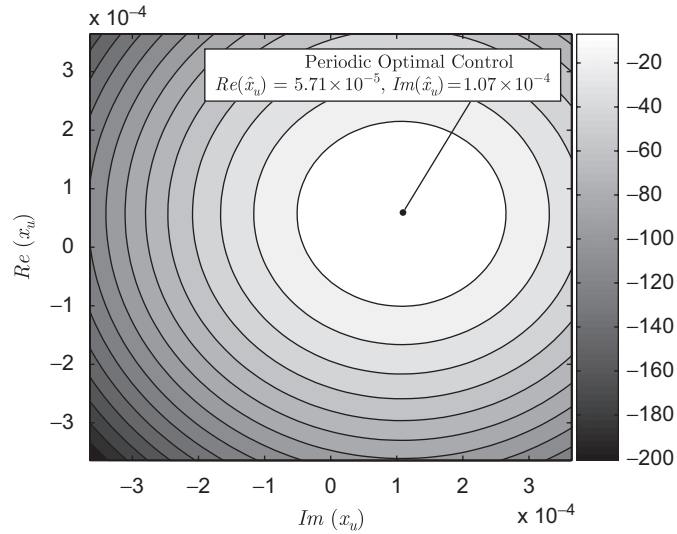
Fig. 8. Contour plot of the normalized energy dissipated per cycle in terms of the real and imaginary parts of x_u for active damping at $r = 0.9$, obtained using the time integration based method.
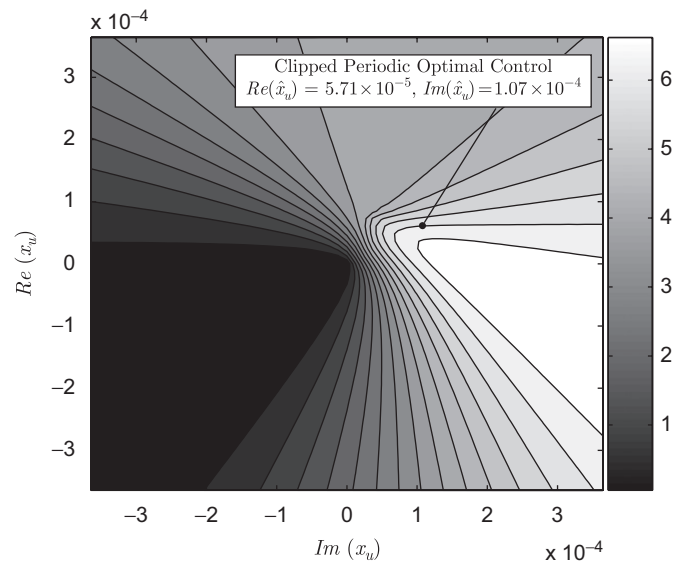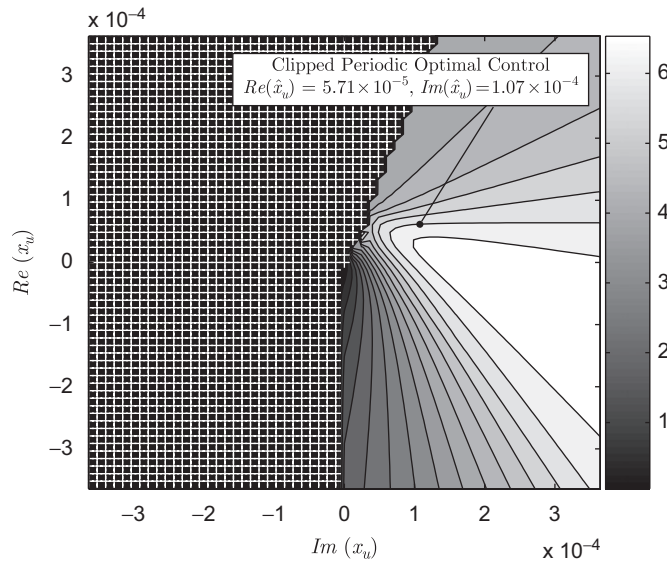

Fig. 9. Contour plot of the normalized energy dissipated per cycle in terms of the real and imaginary parts of x_u for semi-active damping at $r = 0.9$ and $\gamma = 2$, obtained using the time integration based method.

not the "true" optimal form that would require an exact solution.) To answer this question, a contour plot of the normalized energy dissipated per cycle in terms of the real and imaginary parts of x_u was computed using the averaged solution and is shown in Fig. 10. Though it does not allow to compute the normalized energy dissipated per cycle for the entire plane, essentially because Eq. (24) assumes a timing between each harmonic signals, the averaged solution does however enclose the region where, by looking at the figure, one would expect the optimal point to be located. Moreover, for the region where the solution is valid, the plot is very similar to Fig. 9, which was obtained using the time integration procedure. Therefore, this means that, *a priori*, the averaged solution can be used to find $\tilde{x}_u$.

Fig. 10. Contour plot of the normalized energy dissipated per cycle in terms of the real and imaginary parts of x_u for semi-active damping at $r = 0.9$ and $\gamma = 2$, obtained using the averaged solution. The region covered with (▦▦▦) corresponds to a set of values where non-valid solutions were obtained.

5.3. Optimization algorithm for the ICPOC

The idea behind the optimization algorithm of the ICPOC is shown in Fig. 11. The overall optimization criterion to be minimized for the algorithm is

$$J(X_u, \beta) = -\Delta E, \tag{31}$$

where ΔE is given by Eq. (29a), but now considering that X_u and β are allowed to vary so that they are no longer fixed at $\hat{X}_u$ and $\hat{\beta}$. The algorithm essentially involves two imbricated optimization routines. The steps of the algorithm are as follows:

(1) define system parameters: m, k, c, c_{max}, ω and F_{ex};
(2) set boundaries on parameters a, ψ, X_u and β;
(3) give an estimate of X_u and β (first optimization routine);
(4) give an estimate of a and ψ (second optimization routine);
(5) do a and ψ minimize Eq. (28)? If not, go back to step (4);
(6) do X_u and β minimize Eq. (31)? If not, go back to step (3);
(7) end.

The end result of this algorithm will be to give the energy dissipated per cycle by the ICPOC under steady state with the corresponding values of $\tilde{X}_u$ and $\tilde{\beta}$.

5.4. Numerical analysis and discussion on the ICPOC

Fig. 12 presents the normalized energy dissipated per cycle in terms of the frequency ratio for the ICPOC and the corresponding results for the CPOC for $\gamma = 2$. The first observation that can be made from Fig. 12 is that the ICPOC provides a better (or equal for $r = 1$) energy dissipation than the CPOC over the entire span of frequency ratio considered. For the system parameters considered, the relative gain to be made on the energy dissipated over the CPOC is a function of the frequency ratio and it can go as high as 35 percent for $r = 0.7$ and 1.5. This gain will be a function of ζ and γ, where a lower value of ζ and/or a higher value of γ will allow greater energy dissipation.
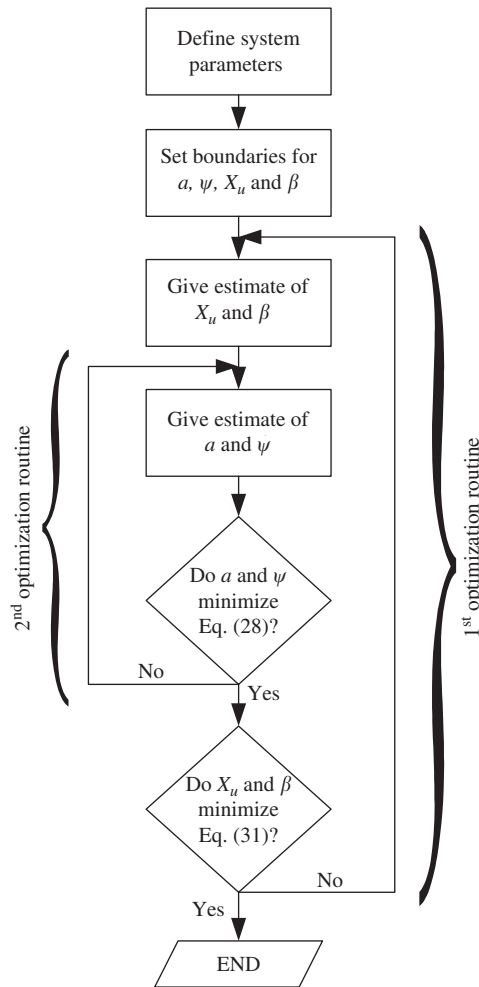
Fig. 11. Optimization algorithm, based on the averaged solution, to determine the energy dissipated per cycle and the improved active effort of the ICPOC.

Figs. 13 and 14 allow to compare the amplitude, $\tilde{X}_u$, and phase, $\tilde{\beta}$, of the ICPOC with the amplitude, $\hat{X}_u$, and phase, $\hat{\beta}$, of the CPOC. We can observe that the amplitude of the ICPOC is different from what is prescribed by the CPOC. One particular aspect of the ICPOC, that can be seen in Fig. 13, is that when r is out of a certain interval, in this case $0.96 \leqslant r \leqslant 1.04$ for $\gamma = 2$, the ICPOC tends to take the form of a Bang–Bang (or On–Off) control since $\tilde{X}_u$ gets very large in comparison to the maximum effort the damper can provide. Also, one can see that when γ is reduced, this phenomenon tends to be more important. This is coherent with the fact that the research on semi-active vibration control has given a lot of attention to the Bang–Bang variety of control approaches [20]. As for the phase plots in Fig. 14, they tend to be similar in shape but the ICPOC prescribes absolute phase values that are larger than the CPOC. A possible explanation to this phenomenon could come from the fact that the ICPOC has only a limited capacity of introducing a "spring-like" or "mass-like" force component to modify the system's dynamics, as opposed to the full capacity of the active damper. Thus, the phase would tend to be larger in order to compensate for this incapacity.

Another interesting aspect of the ICPOC is that $\tilde{X}_u$ and $\tilde{\beta}$, as illustrated in Figs. 13 and 14, are functions of γ. Therefore, an important difference between the CPOC and the ICPOC is that the ICPOC takes the capacity of the semi-active damper into account in the design of the control.
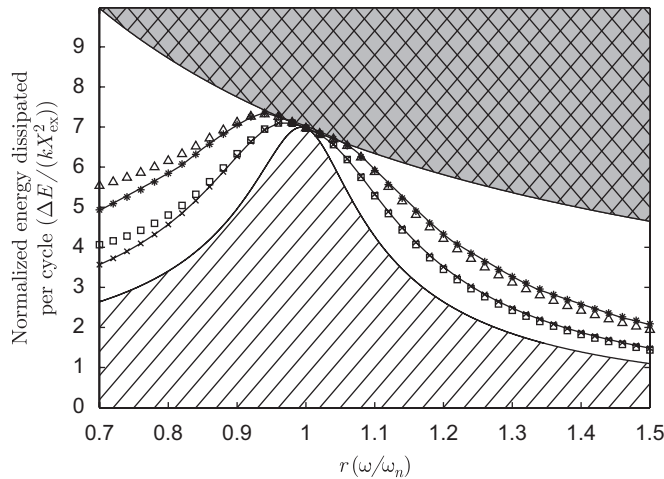
Fig. 12. Normalized energy dissipated per cycle in terms of the frequency ratio obtained from the time integration based method and from the averaged solution for the CPOC and the ICPOC for $\gamma = 2$: ($\longrightarrow\!\times\!\longrightarrow$) averaged solution for the CPOC; ($\square$) time integration for the CPOC; ($\longrightarrow\!\ast\!\longrightarrow$) averaged solution for the ICPOC; ($\triangle$) time integration for the ICPOC.

Fig. 13. Amplitude of the normalized requested effort for the CPOC and the ICPOC: ($\longrightarrow\!\times\!\longrightarrow$) CPOC $\hat{X}_u$; ($\longrightarrow\!\triangleright\!\longrightarrow$) ICPOC $\tilde{X}_u$ for $\gamma = 1.25$; ($\longrightarrow\!\ast\!\longrightarrow$) ICPOC $\tilde{X}_u$ for $\gamma = 2$.

As for the agreement between the approximate solution and the time based simulations results, the results follow the same trend as in Section 4.3 where the agreement between both methods is excellent in the vicinity of $r = 1$, but tends to deteriorate as the frequency ratio gets away from $r = 1$.

In order to verify that the ICPOC could be reduced to a Bang–Bang control when r is out of the interval $0.96 \leqslant r \leqslant 1.04$ for $\gamma = 2$, the Bang–Bang ICPOC control is implemented and can be represented by the following equation:

$$\zeta_{sa} = \begin{cases} \zeta_{\max} & \text{if } \tilde{x}_u \dot{x} \geqslant 0, \\ 0 & \text{otherwise.} \end{cases} \tag{32}$$

The time integration based simulation results for both the ICPOC and the Bang–Bang ICPOC are presented in Fig. 15 for $\gamma = 2$. One can then clearly see that for values of r out of the interval $0.96 \leqslant r \leqslant 1.04$, both controls yield almost identical performance. Indeed, one could probably further improve the performance of the
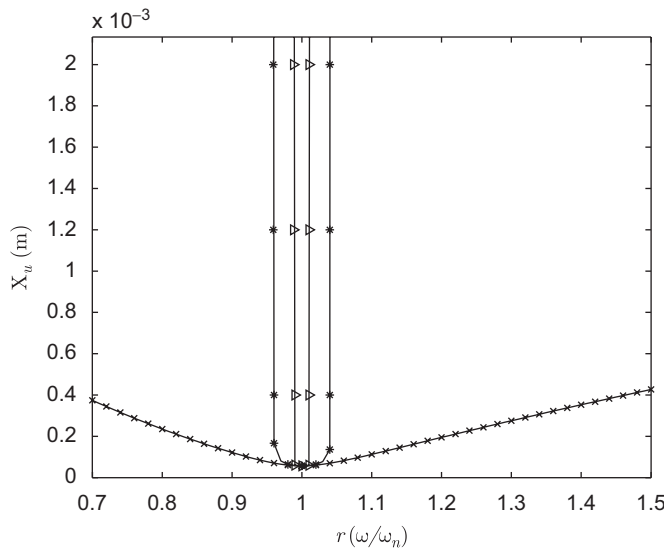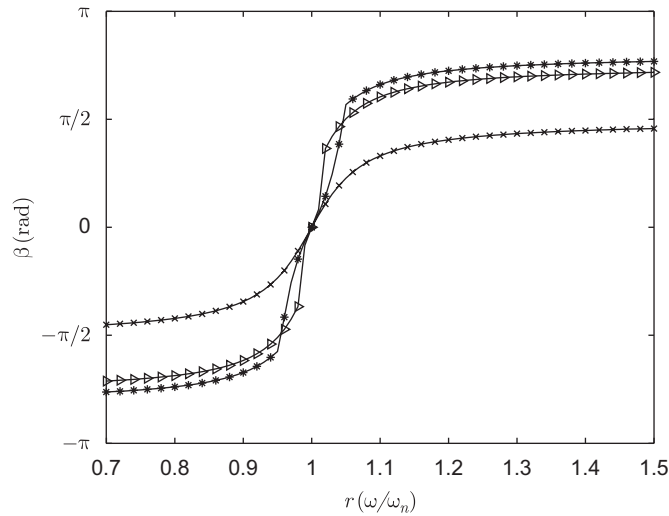
Fig. 14. Phase of the normalized requested effort for the CPOC and the ICPOC: (—✳—) CPOC $\hat{\beta}$; (—▷—) ICPOC $\tilde{\beta}$ for $\gamma = 1.25$; (—✳—) ICPOC $\tilde{\beta}$ for $\gamma = 2$.
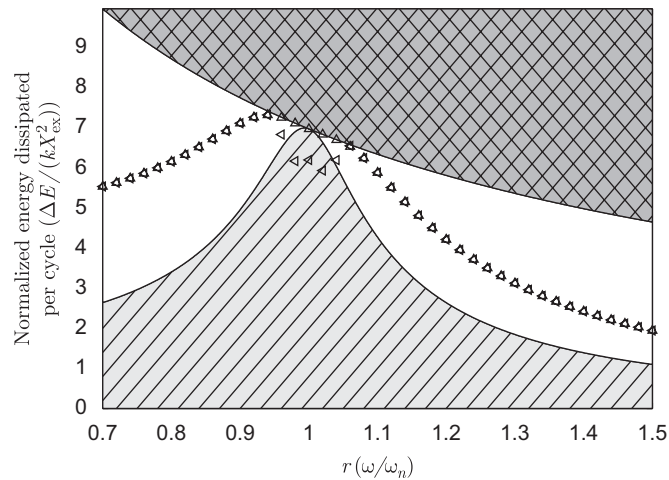

Fig. 15. Normalized energy dissipated per cycle in terms of the frequency ratio obtained from the time integration based method for the ICPOC and the Bang–Bang ICPOC for $\gamma = 2$: (△) time integration for the ICPOC; (◁) time integration for the Bang–Bang ICPOC.

Bang–Bang ICPOC control in the $0.96 \leqslant r \leqslant 1.04$ range by computing the optimal phase of x_u for this particular control, but this is considered to be out of the scope of this paper. This phenomenon opens-up interesting perspectives on future research.

6. Summary and concluding remarks

The purpose of the present paper is to present a new approach to design an effective control law for semi-active harmonic disturbance rejection. To illustrate the approach, the problem of maximizing the energy dissipated per cycle by a semi-actively damped SDOF system was treated. In order to establish a base of comparison between the semi-active damper and its passive and active counterparts, the analytical results for the energy dissipated per cycle at optimal by a passive damper and an active damper (obtained by Kasturi and Dupont [19]) are first presented.

As a starting point for the design of the new control law, the clipped optimal control approach was used, which essentially involves designing a control law that allows the semi-active damper to generate an effort that

follows, "at best", the requested effort of the active optimal case. For the problem considered in this paper, the approach yields a control law that was called the "clipped periodic optimal control" (or CPOC). In order to determine the ability of the CPOC to improve the energy dissipation capacity of the semi-active damper over the passive optimal damper, an approximate solution to the nonlinear dynamic problem was obtained using the method of averaging and a time integration based method was proposed. The key observations of the CPOC are as follows:

(1) The CPOC allows to improve the energy dissipated per cycle by the semi-active damper over the optimal passive damper for the entire span of frequency ratio considered (except at $r = 1$ where there is no room for improvement).
(2) The CPOC yields a control effort that is periodic at twice the frequency of the excitation, which is coherent with the paper presented by Anusonti-Inthra and Gandhi [4].

The main originality of this paper is then to "improve", or "fine tune", the result obtained from the clipped optimal control approach in order to obtain an "improved clipped periodic optimal control" (or ICPOC). This is done using the same control law as the CPOC but varying the requested effort signal which is no longer constrained to its active optimal form. The new parameters for the requested effort are found using the approximate solution to the CPOC problem and an appropriate optimization algorithm. The main findings resulting from the ICPOC are:

(1) The ICPOC offers increased performance over the CPOC for the entire span of frequency considered (or equal at $r = 1$).
(2) The new approach developed allows to implicitly take into account the modulation capacity of the semi-active damper in the determination of the control parameters as opposed to the clipped optimal control approach, which is independent of the modulation capacity of the semi-active damper.
(3) As the frequency ratio gets away from resonance, the ICPOC takes the form of a Bang–Bang (or On–Off) control, which is coherent with the large amount of attention that this variety of control has received for semi-active vibration control [20].

Overall, it was shown that considerable gains can be made by using the approach presented in this paper over the already established clipped optimal control approach.

6.1. Future work

The approach developed in this paper opens up many opportunities for future research. For example, interesting insights could be obtained by using the approach to synthesize an effective control law for the semi-active vibration isolation problem. Also, the results presented in this paper suggested that, as r gets away from resonance, a Bang–Bang (or On–Off) control logic could give similar performance to the ICPOC. This aspect should be analyzed more thoroughly because of the relative simplicity that a Bang–Bang control law offers for practical implementation.

References

[1] D.J. Inman, *Engineering Vibration*, second ed., Prentice-Hall, New Jersey, 2001.
[2] A.D. Nashif, D.I.G. Jones, J.P. Henderson, *Vibration Damping*, Wiley, New York, 1985.
[3] S.E.C.R. Fuller, P.A. Nelson, *Active Control of Vibration*, Academic Press, San Diego, CA, 1996.

  [4] P. Anusonti-Inthra, F. Gandhi, Cyclic modulation of semi-active controllable dampers for tonal vibration isolation, *Journal of Sound and Vibration* 275 (1–2) (2004) 107–126.
  [5] H.P. Gavin, A. Zaicenco, Performance and reliability of semi-active equipment isolation, *Journal of Sound and Vibration* 306 (1–2) (2007) 74–90.
  [6] Y. Shen, M. Golnaraghi, G. Heppler, Semi-active vibration control schemes for suspension systems using magnetorheological dampers, *JVC/Journal of Vibration and Control* 12 (1) (2006) 3–24.
  [7] M.A. Karkoub, M. Zribi, Active/semi-active suspension control using magnetorheological actuators, *International Journal of Systems Science* 37 (1) (2006) 35–44.
  [8] G. Georgiou, G. Verros, S. Natsiavas, Multi-objective optimization of quarter-car models with a passive or semi-active suspension system, *Vehicle System Dynamics* 45 (1) (2007) 77–92.
  [9] M.D. Symans, M.C. Constantinou, Semi-active control systems for seismic protection of structures: a state-of-the-art review, *Engineering Structures* 21 (6) (1999) 469–487.
 [10] K.A. Bani-Hani, M.A. Sheban, Semi-active neuro-control for base-isolation system using magnetorheological (MR) dampers, *Earthquake Engineering and Structural Dynamics* 35 (9) (2006) 1119–1144.
 [11] G.M. Fabio Casciati, F. Marazzi, *Technology of Semiactive Devices and Applications in Vibration Mitigation*, first ed., Wiley, UK, 2006.
 [12] P. Dupont, P. Kasturi, A. Stokes, Semi-active control of friction dampers, *Journal of Sound and Vibration* 202 (2) (1997) 203–218.
 [13] D. Karnopp, M.J. Crosby, R.A. Harwood, Vibration control using semi-active force generators, *Journal of Engineering for Industry, Transactions of the ASME, Series B* 96 (2) (1974) 619–626.
 [14] M. Setareh, J.K. Ritchey, T.M. Murray, J.-H. Koo, M. Ahmadian, Semiactive tuned mass damper for floor vibration control, *Journal of Structural Engineering* 133 (2) (2007) 242–250.
 [15] M. Neubauer, R. Oleskiewicz, K. Popp, T. Krzyzynski, Optimization of damping and absorbing performance of shunted piezo elements utilizing negative capacitance, *Journal of Sound and Vibration* 298 (1–2) (2006) 84–107.
 [16] J.S. Lane, A.A. Ferri, B.S. Heck, *Vibration Control using Semi-active Friction Damping*, Vol. 49, ASME, Design Engineering Division, Anaheim, CA, USA, 1992, pp. 165–171.
 [17] T. Pinkaew, Y. Fujino, Effectiveness of semi-active tuned mass dampers under harmonic excitation, *Engineering Structures* 23 (7) (2001) 850–856.
 [18] K. Wang, Y. Kim, D. Shea, Structural vibration control via electrorheological-fluid-based actuators with adaptive viscous and frictional damping, *Journal of Sound and Vibration* 177 (2) (1994) 227–237.
 [19] P. Kasturi, P. Dupont, Constrained optimal control of vibration dampers, *Journal of Sound and Vibration* 215 (3) (1998) 499–509.
 [20] Y. Liu, T. Waters, M. Brennan, A comparison of semi-active damping control strategies for vibration isolation of harmonic disturbances, *Journal of Sound and Vibration* 280 (1–2) (2005) 21–39.
 [21] P. Buaka, P. Micheau, P. Masson, *A Semi-active Friction Device Controlled by Nonlinear Feedbacks and Phase-shift Compensation*, Active 2006, Adelaide, Australia, 2006.
 [22] P.D. Mitcheson, T.C. Green, E.M. Yeatman, A.S. Holmes, Architectures for vibration-driven micropower generators, *Journal of Microelectromechanical Systems* 13 (3) (2004) 429–440.
 [23] P. Buaka, P. Masson, P. Micheau, Determination of normal force for optimal energy dissipation of harmonic disturbance in a semi-active device, *Journal of Sound and Vibration* 311 (3) (2008) 633–651.
 [24] J. Lagarias, J. Reeds, M. Wright, P. Wright, Convergence properties of the Nelder–Mead simplex method in low dimensions, *SIAM Journal on Optimization* 9 (1) (1998) 112–147.
 [25] L. Gaul, H. Albrecht, J. Wirnitzer, Semi-active friction damping of large space truss structures, *Shock and Vibration* 11 (3–4) (2004) 173–186.